

## ORIGINAL ARTICLE

# Characterizing affinity epitopes between prion protein and $\beta$ -amyloid using an epitope mapping immunoassay

Mino Kang<sup>1</sup>, Su Yeon Kim<sup>2</sup>, Seong Soo A An<sup>1</sup> and Young Ran Ju<sup>2</sup>

Cellular prion protein, a membrane protein, is expressed in all mammals. Prion protein is also found in human blood as an anchorless protein, and this protein form is one of the many potential sources of misfolded prion protein replication during transmission. Many studies have suggested that  $\beta$ -amyloid<sub>1-42</sub> oligomer causes neurotoxicity associated with Alzheimer's disease, which is mediated by the prion protein that acts as a receptor and regulates the hippocampal potentiation. The prevention of the binding of these proteins has been proposed as a possible preventative treatment for Alzheimer's disease; therefore, a greater understanding of the binding hot-spots between the two molecules is necessary. In this study, the epitope mapping immunoassay was employed to characterize binding epitopes within the prion protein and complementary epitopes in  $\beta$ -amyloid. Residues 23–39 and 93–119 in the prion protein were involved in binding to  $\beta$ -amyloid<sub>1-40</sub> and <sub>1-42</sub>, and monomers of this protein interacted with prion protein residues 93–113 and 123–166. Furthermore,  $\beta$ -amyloid antibodies against the C-terminus detected bound  $\beta$ -amyloid<sub>1-42</sub> at residues 23–40, 104–122 and 159–175.  $\beta$ -Amyloid epitopes necessary for the interaction with prion protein were not determined. In conclusion, charged clusters and hydrophobic regions of the prion protein were involved in binding to  $\beta$ -amyloid<sub>1-40</sub> and <sub>1-42</sub>. The 3D structure appears to be necessary for  $\beta$ -amyloid to interact with prion protein. In the future, these binding sites may be utilized for 3D structure modeling, as well as for the pharmaceutical intervention of Alzheimer's disease.

*Experimental & Molecular Medicine* (2013) 45, e34; doi:10.1038/emm.2013.63; published online 2 August 2013

**Keywords:** Alzheimer's disease; amyloid- $\beta$ ; epitope mapping; ligand; prion protein

## INTRODUCTION

The cellular prion protein (PrPC) is a membrane protein with a glycosylphosphatidylinositol anchor that is expressed in all mammals. PrPC is also found in blood as an anchorless protein.<sup>1</sup> The accumulation of the toxic misfolded infectious form of the prion protein in the brain is a well-known characteristic of transmissible spongiform encephalopathies, which are better known as prion diseases.<sup>2</sup> Although the PrPC to misfolded prion protein conversion mechanism has not been clearly determined, conformational changes in the protein structure that transform  $\alpha$ -helices to  $\beta$ -sheets were observed using circular dichroism analysis.<sup>3</sup>

Several functions of PrPC were suggested in the absence of clear knowledge of the role of PrPC, and PrPC knockout mice did not display any noticeable defects during their growth and development.<sup>4,5</sup> Interestingly, a previous study of the <sup>23</sup>KKRPKPGGW<sup>31</sup> region in the PrPC peptide suggested that this region contains a neuroprotective functional moiety.<sup>6</sup>

Other protective roles of PrPC were suggested by other groups in experiments involving Bax overexpression,<sup>7,8</sup> oxidative stress<sup>9,10</sup> and mitochondrial dysfunction induced by serum deprivation.<sup>11</sup> Furthermore, amino acids 106–126 of PrPC comprise a short toxic peptide sequence that mimics misfolded prion protein aggregation.<sup>12</sup> Overall, PrPC may be involved in the neuroprotective and neurotoxic functions, but the effects remain unclear.<sup>13</sup>

Similar to the misfolded prion protein pathogenic protein,  $\beta$ -amyloid<sub>1-42</sub> (A $\beta$ 42) has been shown to be involved in Alzheimer's disease (AD). AD is a neurodegenerative disorder that accompanies memory loss and impaired cognitive function. Clinically, the accumulation of A $\beta$  in senile plaques and the hyperphosphorylation of Tau protein in neurofibrillary tangles in the brain are representative hallmarks of AD patients.<sup>14–16</sup> During AD pathogenesis, A $\beta$  accumulation is considered to be the first mechanism of progression, which is based on observed cognitive impairments followed by

<sup>1</sup>Department of Bionanotechnology, Gachon University, Gyeonggi, Korea and <sup>2</sup>Division of Zoonoses, Center for Immunology and Pathology, National Institute of Health, Korea Centers for Disease Control and Prevention, Osong, Republic of Korea

Correspondence: Professor SSA An, Department of Bionanotechnology, Gachon University, 65 San, Bokjeong-dong, Sujeong-gu, Seongnam-si, Gyeonggi-do 461-701, South Korea.

E-mail: seong.an@gmail.com

Received 23 December 2012; revised 12 April 2013; accepted 2 May 2013

intraneuronal A $\beta$  accumulation.<sup>17</sup> Therefore, A $\beta$  aggregation is considered to be the most pathogenic process in AD.<sup>18–23</sup>

The production of A $\beta$ 42 results from  $\beta$ - and  $\gamma$ -secretase-mediated cleavage of the amyloid precursor protein.<sup>24</sup> This 42-amino-acid peptide spontaneously aggregates, which creates toxic plaques in the brain.<sup>25</sup> However, the mechanisms of the amyloid cascade remain unclear due to the lack of correlation between the number of plaques and cognitive decline.<sup>26,27</sup> Among heterogeneous conformations of A $\beta$ 42 (monomers, oligomers and fibrils), oligomeric A $\beta$ 42 has been suggested to be the primary cause of AD.<sup>28–32</sup> Soluble A $\beta$ 42 oligomers have been strongly correlated with synaptic loss, as well as the accumulation of intracellular A $\beta$  in AD pathophysiology.<sup>33</sup>

The toxic mechanisms mediated by A $\beta$  oligomers during AD pathogenesis have still not been elucidated. Various A $\beta$  oligomer structures that form in the extracellular matrix may induce apoptotic cell death and oxidative stresses by interacting with various receptors such as the pan-specific p75 neurotrophin receptor,<sup>34</sup> the N-Methyl-D-aspartate-type glutamate receptor,<sup>35</sup> the Frizzled receptor<sup>36</sup> and the insulin receptor.<sup>37</sup> However, membrane-bound PrPC, which is a receptor for A $\beta$  oligomers, was suggested to be involved in regulating long-term potentiations in the hippocampus that were induced by oligomeric A $\beta$ 42.<sup>38</sup> Furthermore, the binding of A $\beta$ 42 oligomers to PrPC was inhibited when 6D11, an anti-PrPC antibody against the epitope containing amino acids 93–109, was used to treat the cells expressing PrPC.<sup>39</sup> These studies indicate the potential role of PrPC as a receptor that mediates the toxic effects of A $\beta$ 42 oligomers. In contrast, other studies have suggested that PrPC-mediated A $\beta$ 42 oligomer toxicity may not be the only mechanism that causes its toxicity.<sup>40,41</sup>

In previous studies, the binding sites in PrPC that mediate the interaction with A $\beta$ 42 were analyzed using competitive antibody assays<sup>39</sup> and surface plasmon resonance.<sup>40</sup> Nuclear magnetic resonance (NMR) and the simulation of a PrPC and A $\beta$ 42 docking model suggested that both A $\beta$ 42 monomers and dimers bind to a similar site in PrPC.<sup>42</sup> Antibody or protein–protein interaction epitope mapping using multiple overlapping peptides has been widely applied, and a large amount of research data has been accumulated. Therefore, resources such as SPOTs synthesis<sup>43</sup> (Sigma's custom SPOTs service) and other similar methods (for example, the pin-bound peptides method<sup>44</sup> and free peptide assays<sup>45</sup>) are already available.

In the present study, the PrPC epitopes involved in A $\beta$ 42 binding were investigated using epitope mapping immunoassays. The principles of this method and its applications are introduced throughout this paper. We determined that PrPC binds to A $\beta$ 40 in addition to A $\beta$ 42, which was previously reported. Through experimentation, we determined that the 3D structure of A $\beta$ 42 appeared to be important for the binding to PrPC. The investigation of PrP and A $\beta$  interaction sites provides a greater understanding of the actions of PrPC as a receptor and assists in the development of immunoassay diagnostic tools and the creation of pharmaceutical interventions for AD.

## MATERIALS AND METHODS

All overlapping peptides were synthesized using Fmoc solid-phase peptide synthesis from Anygen (Jeollanam-do, South Korea), with approximately 90% purity. His-tagged PrPC (human) was purified from *Escherichia coli* using Ni-NTA agarose beads,<sup>46</sup> and A $\beta$ 40 and A $\beta$ 42 were purchased from Bachem (Bubendorf, Switzerland). SAF-32 antibody purchased from Cayman Chemical (Ann Arbor, MI, USA) and 6D11, 1E11, 6E10 and 4G8 antibodies obtained from Signet Laboratories (Dedham, MA, USA) were used to test the efficacy of the epitope mapping enzyme-linked immunosorbent assay (EpiMap ELISA) tests, depending on their respective antigens. Horseradish peroxidase (HRP)-conjugated anti-PrPC antibody was kindly provided by Dr T. Yokoyama,<sup>47</sup> and biotin-conjugated A $\beta$ 42 antibody against the C-terminus (6D5) was purchased from US Biological (Swampscott, MA, USA). Maleimide-activated microplates were used to conjugate the overlapping peptides to cysteine residues. HRP-conjugated NeutrAvidin and salmon serum albumin (SeaBlock) were purchased from Thermo Scientific (Rockford, IL, USA). Additionally, 96-well black MaxiSorp plates were purchased from Nunc (#475515, Roskilde, Denmark). Phosphate-buffered saline (PBS), PBS with 0.05% Tween 20 (PBST), Tris-buffered saline with 0.05% Tween 20 (TBST), ethylenediaminetetraacetic acid, HRP-conjugated goat anti-mouse IgG, dimethyl sulfoxide (DMSO) and 3,3',5,5'-tetramethylbenzidine were purchased from Sigma-Aldrich (St Louis, MO, USA). Dynabeads M-280 Tosylactivated magnetic beads were purchased from Invitrogen (Oslo, Norway). BLOCK ACE (AbD Serotec, Raleigh, NC, USA) was dissolved in distilled water to make a 4% solution.

### The preparation of the PrPC and A $\beta$ 42 EpiMap ELISA tests

Both human PrPC and A $\beta$ 42 sequences were obtained from the universal protein resource knowledgebase (UniProtKB). Forty-four overlapping 17-mer peptides were synthesized by shifting three amino acids from the N- to C-terminus of the PrPC sequence, where each peptide was numbered consecutively. These peptides were generated with a cysteine at the end of the N- or C-terminus of each peptide, except for the peptides numbered 29, 30, 31, 32, 33, 41, 42, 43 and 44 because their inner cysteine residue was used. The peptides numbered 10, 12, 13, 18 and 39 failed to be synthesized due to aggregation problems, and partial sequences of the octapeptide repeat region were omitted (Figure 1a).

The human A $\beta$ 42 sequence from UniProt was used to design 15-mer peptides from the N- to C-terminus of A $\beta$ 42. A cysteine residue was designed at the C-terminus of the peptides numbered 1–8 and the N-terminus of the peptides 9–16 (Figure 1b). Unfortunately, peptide 15 could not be synthesized due to an aggregation problem. The cysteine residue provided a sulfhydryl group to link the peptides on the plate through a maleimide reaction. A schematic description of the EpiMap ELISA preparation is presented in Figure 2.

This protocol was designed on the basis of the manufacturer's instructions. All peptides were solubilized in DMSO at high concentrations and were then further diluted in PBS (pH 4.5) to prevent dimerization. Peptides were reconstituted to 5  $\mu\text{g ml}^{-1}$  in PBS (pH 7.2) containing 10 mM ethylenediaminetetraacetic acid and were immediately added to the maleimide-activated 96-well plates (100  $\mu\text{l}$  per well). Next, the peptides were incubated overnight at 4  $^{\circ}\text{C}$  and blocked using 10  $\mu\text{g ml}^{-1}$  of cysteine (200  $\mu\text{l}$  per well) for the remaining maleimide groups. The plates were then washed three times with 300  $\mu\text{l}$  of PBST (pH 7.4).

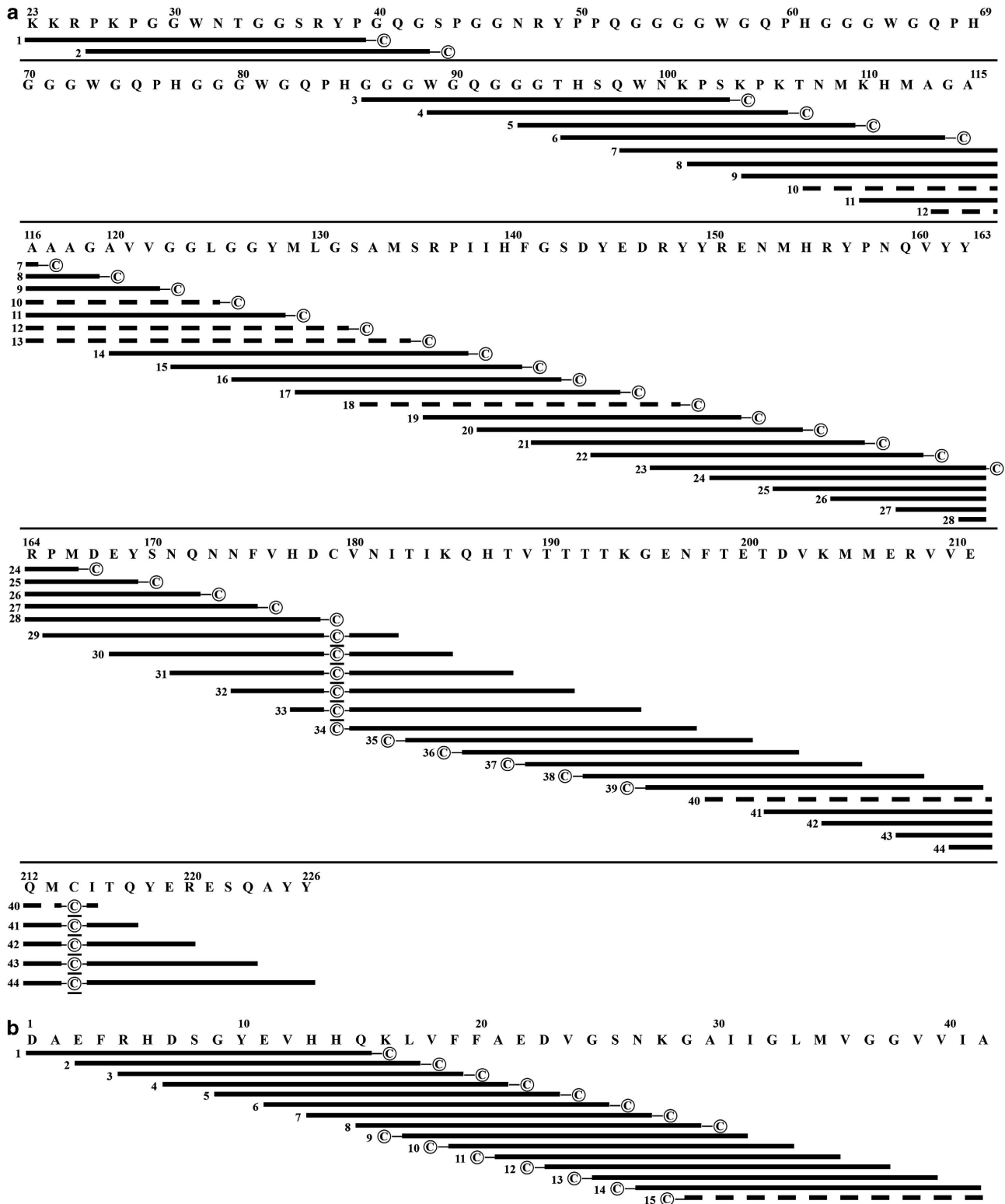


**Figure 1** Schematic figures of (a) cellular prion protein and (b)  $\beta$ -amyloid<sub>1-42</sub> overlapping peptides. Each black bar represents overlapping peptides and their locations, while -C indicates the cysteine residue used for peptide conjugation.

### The evaluation of the PrPC and A $\beta$ 42 EpiMap ELISA tests

The PrPC monoclonal antibodies with known epitopes such as SAF-32 (epitopes, 57–88), 6D11 (epitopes, 91–109), A $\beta$ 42 antibodies (1E11 (epitopes, 1–8) and HRP-conjugated 4G8 (epitopes, 17–25))

were used to assess the epitope mapping potential of the EpiMap ELISA. Antibodies were reconstituted to 0.01  $\mu\text{g ml}^{-1}$  in TBST (pH 8.0) with 0.4% BLOCK ACE. After a 1-h incubation period, each well was washed three times in 300  $\mu\text{l}$  of TBST. The HRP-conjugated

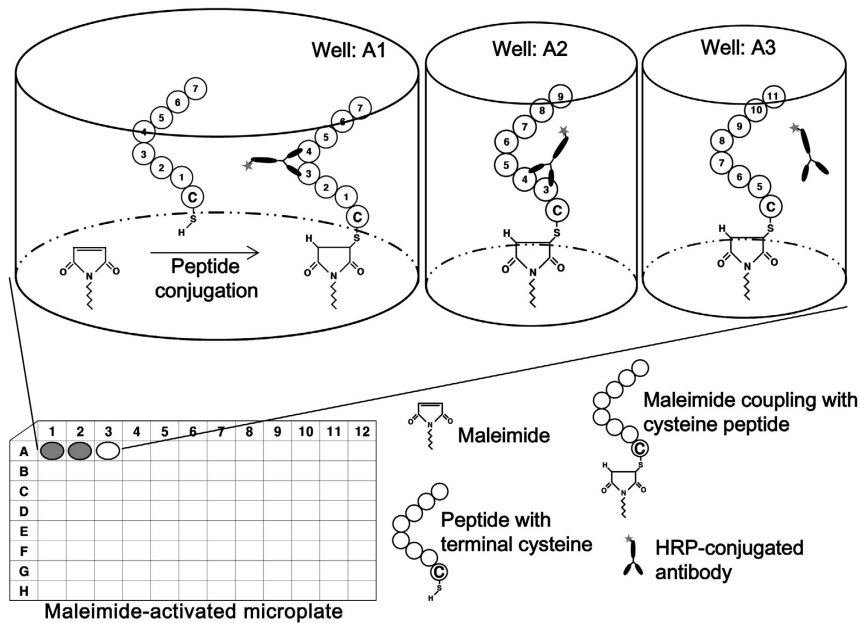


**Figure 2** The principles of overlapping peptide conjugation and epitope mapping strategies. A sulfhydryl group from a cysteine at the end of each overlapping peptide was conjugated through a maleimide reaction onto a maleimide-activated plate. If the antibody targeted amino acids 3 and 4 of the peptide, the antibody detected overlapping peptides that contained the same epitopes. The overlapping peptide in Well:A3 did not contain amino acids 3 and 4; therefore, the antibody did not bind to the overlapping peptide. Therefore, no enzymatic chemical changes occurred in Well:A3 (presented as blanked circle). Increased absorbances were observed in Well:A1 and Well:A2 (presented as gray circles), which was then calculated to identify significant binding epitopes. In addition to antibody epitope mapping, protein–protein interaction sites were identified using the same principle.

anti-mouse IgG antibody (1:5000) was added, and the mixture was incubated for 1 h at 37 °C followed by three washes in TBST. An HRP signal was visualized by determining the absorbance at 450 nm after sequential additions of 3,3',5,5'-tetramethylbenzidine (100  $\mu$ l per well) and sulfuric acid (50  $\mu$ l, 2 N).

### $\beta$ -amyloid preparation and electrophoresis

A $\beta$ 40 and A $\beta$ 42 in lyophilized form were dissolved in DMSO. A $\beta$  in DMSO was further diluted in PBS to a final amount of 5  $\mu$ g and incubated for 2 h at 37 °C before electrophoresis. Mini-PROTEAN Tris-Tricine precast gels (10–20%) from Bio-Rad Laboratories (Hercules, CA, USA) were prepared with 1X cathode buffer (0.1 M Tris, 0.1 M Tricine, 0.1% SDS and pH 8.3) in the top chamber of the gel and 1X anode buffer (0.2 M Tris, pH 8.9) in the bottom chamber. The proteins were separated in an iced chamber at 150 V, and silver staining was performed (Pierce # 24612, Rockford, IL, USA).

### Protein epitope mapping with EpiMap ELISA

Overall, 42-amino-acid sequences in PrPC were predicted to be involved in the interaction with A $\beta$ 40 by applying 0.1  $\mu$ g ml<sup>-1</sup> of A $\beta$ 420 and by using the PrPC EpiMap ELISA plate (100  $\mu$ l per well). After 1 h at 37 °C, each well was washed three times with 300  $\mu$ l of PBST, and anti-A $\beta$ 42 (6E10) HRP-conjugated antibodies were applied at 0.1  $\mu$ g ml<sup>-1</sup> in PBST with 0.4% BLOCK ACE. For the 6D5 biotinylated antibody, 0.1  $\mu$ g ml<sup>-1</sup> was applied under the same conditions, and NeutrAvidin–HRP (1:5000) was added after three consecutive washes. In another A $\beta$ 42 EpiMap ELISA experiment, PrPC reconstituted with PBST (0.1  $\mu$ g ml<sup>-1</sup>, 100  $\mu$ l per well) was applied to A $\beta$ 42 EpiMap ELISA plate and incubated for 1 h at 37 °C. After three washes with 300  $\mu$ l of PBST, the anti-PrP antibodies (T2 or

SAF-32) were applied at 0.1  $\mu$ g ml<sup>-1</sup> in PBST with 0.4% BLOCK ACE. After 1 h of incubation, the microplates were washed three times with PBST. Subsequently, 3,3',5,5'-tetramethylbenzidine (100  $\mu$ l per well) was applied to both EpiMap ELISA plates and was incubated for 20 min. Finally, the reaction was quenched with H<sub>2</sub>SO<sub>4</sub> (50  $\mu$ l, 2 N).

### The recombinant PrPC and A $\beta$ 42 interaction

The recombinant PrPC and A $\beta$ 42 proteins were conjugated to Tosylactivated magnetic beads following the manufacturer's protocol (Invitrogen, Oslo, Norway). Briefly, 1  $\mu$ M of each protein in phosphate buffer (0.1 M) was incubated with magnetic beads ( $4 \times 10^8$  beads) for 24 h at 37 °C. Non-specific binding was reduced by incubating in 1% BLOCK ACE for 4 h. Approximately,  $4 \times 10^6$  beads in 50  $\mu$ l were used for each sample, and 100  $\mu$ l of PrPC (10 ng ml<sup>-1</sup>) was used for the binding experiments. The final volume of the assay was fixed to 200  $\mu$ l by adding TBST (pH 8.0). In the assay, PrPC was added to A $\beta$ 42- and BA-conjugated magnetic beads where HRP-conjugated anti-PrPC (0.1  $\mu$ g ml<sup>-1</sup>) detected any bound PrPC. For negative controls, A $\beta$ 42- and BA-conjugated magnetic beads were incubated with PrPC antibody, while PrPC-conjugated magnetic beads were used as a positive control. Enhanced chemiluminescence HRP substrate (200  $\mu$ l) was added, and the luminescence signals were measured with a Victor<sup>3</sup> multi-spectrophotometer (Perkin Elmer, Boston, MA, USA) in relative luminescence units (RLU).

### Statistical analysis

All assays were performed in triplicate, and quantitative data were compared among the groups using Student's *t*-test in MiniTab version 14 (Minitab Inc., State College, PA, USA). The differences were considered to be significant at  $P \leq 0.05$ . Data analysis for epitope

mapping adapted guidelines from a previous review paper.<sup>48</sup> First, the average absorbance detected from each overlapping peptide was determined and was subtracted by the lowest quartile (25%) to provide the corrected data. Second, the corrected data were divided by the mean of average absorbance from all peptides to generate normalized data (in  $\sigma$  units). These normalized data were assigned to each overlapping peptide; therefore, each amino acid in the overlapping peptides was allocated with the same normalized data obtained from the overlapping peptides. At last, these normalized data were assigned to the amino acids that belong to the overlapping peptide. The amino acids from the first overlapping peptide overlap with one another; therefore, the normalized data that indicated the same amino acids were summed to provide the 'sum of normalized activity'. The data above 5  $\sigma$  units were considered to be positive with a good degree of confidence based on the previous review paper.<sup>48</sup>

## RESULTS

### The preparation of PrPC and A $\beta$ 42 EpiMap ELISA tests

The EpiMap ELISA was prepared from an array of synthetic peptides on 96-well microtiter plates using 44 overlapping peptides (17 mer) from the N- to C-terminus of the PrPC sequence (Figure 1a). Using the A $\beta$ 42 EpiMap ELISA, 15 overlapping peptides (15 mer) from the N- to C-terminus of A $\beta$ 42 (Figure 1b) were synthesized and immobilized onto 96-well plates. Overlapping peptides were synthesized with a cysteine residue at the N- or C-terminal ends to conjugate on the maleimide-activated microplates through their free sulfhydryl group. Increased hydrophobicity of overlapping peptides was anticipated with the addition of a cysteine. Unfortunately, the PrPC peptides no. 10, 12, 13, 18 and 40

could not be purified because they formed aggregates upon release from the solid-phase peptide synthesis beads. Regarding the A $\beta$ 42 overlapping peptides, peptide no. 15 was also lost due to aggregation. The overlapping peptides were conjugated to a maleimide-activated microplate through a cysteine residue. A schematic explanation of the overlapping peptide conjugation as well as the basic principle of the EpiMap ELISA test is explained in Figure 2.

### The evaluation of PrPC and A $\beta$ 42 EpiMap ELISA tests

Well-characterized commercial PrPC antibodies with the known epitopes, SAF-32 and 6D11, were applied to the PrPC EpiMap ELISA for validation. The SAF-32 epitope (residues 59–89) or the octapeptide repeat region of PrPC<sup>49</sup> were analyzed by the PrPC EpiMap ELISA and showed significant binding (> 5  $\sigma$  units) in regions 26–42 and 86–103 (Figure 3a). The end of the octapeptide repeat region was detected with SAF-32; however, the repeat region was omitted in the PrPC EpiMap ELISA. Another PrPC antibody, 6D11 (epitope 93–109<sup>50</sup>), was tested using the same procedure. Absorbance was measured at 450 nm and was calculated as the sum of normalized data to identify the binding epitope. The PrPC residues 89–116 were found to have significant binding (> 5  $\sigma$  units) (Figure 3b).

A microplate that conjugated with A $\beta$ 42 overlapping fragments (A $\beta$ 42 EpiMap ELISA) was validated with A $\beta$ 42-specific antibodies, 1E11 (residues 1–8; Covance) and 4G8 (residues 17–24; Covance). Based on the A $\beta$ 42 EpiMap ELISA, 1E11 and 4G8 were found to be significantly reactive (> 5  $\sigma$  units)

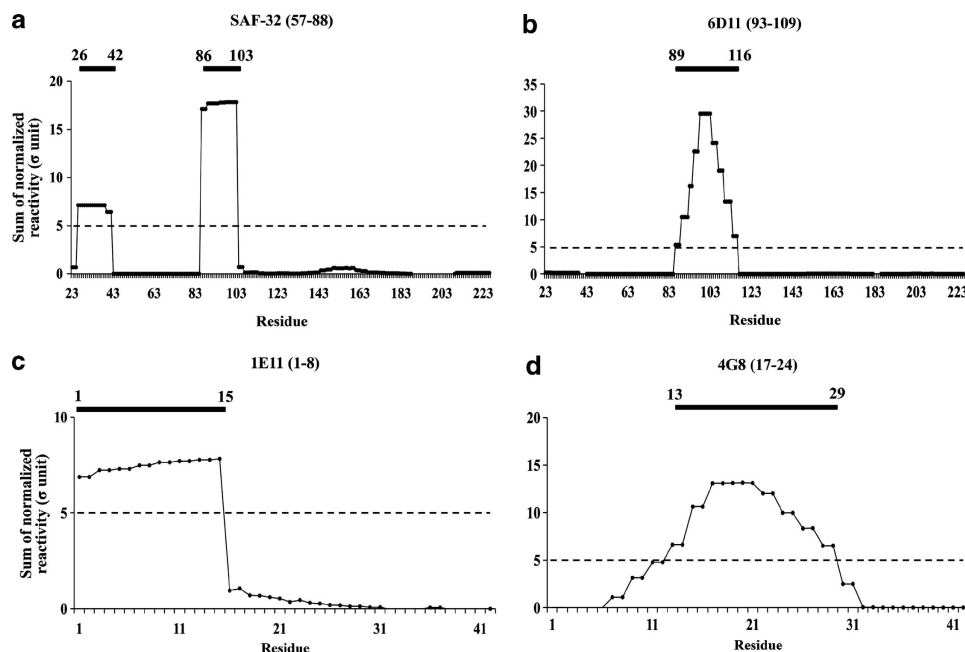


**Figure 3** Epitope-known cellular prion protein (PrPC) antibodies: (a) SAF-32 antibody and (b) 6D11, and  $\beta$ -amyloid<sub>1-42</sub> (A $\beta$ 42) antibodies (c) 1E11 and (d) 4G8 were tested in PrPC or A $\beta$ 42 epitope mapping enzyme-linked immunosorbent assay (EpiMap ELISA) experiments. The known epitopes of the antibodies are indicated adjacent to the name of the antibody in brackets. The X axis of a and b shows the PrPC amino acid number, while c and d are the A $\beta$ 42 amino acid number. The sum of normalized reactivity, which is calculated based on the absorbance of each overlapping peptide, is represented as the Y axis. The black bar and number indicate the binding epitopes of the antibodies that were used in the EpiMap ELISA experiment.

to residues 1–15 and 13–29 of A $\beta$ 42, respectively (Figures 3c and d). These validation experiments using EpiMap ELISA with well-characterized SAF-32, 6D11, 1E11 and 4G8 suggest its potential benefits in characterizing other specific binding interactions with PrPC or A $\beta$ 42.

### Protein epitope mapping with the EpiMap ELISA

The synthetic A $\beta$ 40 and A $\beta$ 42 used in this experiment showed different results. The majority of A $\beta$ 40 isoforms consisted of monomers; however, A $\beta$ 42 isoforms consisted of monomers to tetramers in Tris-Tricine non-denaturing electrophoresis (Figure 4a). A $\beta$ 42-binding epitopes in PrPC were elucidated using the PrPC EpiMap ELISA with recombinant A $\beta$ 42 and 6E10 antibodies (Figure 4b). A previous study by Lauren *et al.*<sup>39</sup> reported that residues 95–110 of the PrPC sequence were necessary for A $\beta$ 42 binding. The N-terminal region of PrPC was also suggested to be involved in mediating binding by another study.<sup>40</sup> Our PrPC EpiMap ELISA showed that epitopes 93–119 as well as 23–39 were involved in binding, as previously reported. Similarly, when synthetic A $\beta$ 40 was applied, and the bound peptides were detected by the 6E10-HRP antibody, the sum of normalized data from the PrPC EpiMap ELISA confirmed the involvement of the 93–113 and 123–166 epitopes. The N-terminal region showed weak binding that was not found to be significant (Figure 4d). The N-terminus-specific 6E10 A $\beta$ 42 antibody was successfully used to detect bound A $\beta$ 42; therefore, the C-terminal-specific antibody, 6D5, was also tested in a similar manner. When

bound A $\beta$ 42 was detected by 6D5, significant interactions occurred at residues 23–40, 104–122 and 159–175 (Figure 4c).

The recombinant PrPC was applied to the A $\beta$ 42 EpiMap ELISA to locate its A $\beta$ 42 binding epitope. PrPC was detected by T2 or SAF-32 PrPC antibodies; however, no notable binding was detected (data not shown). Other combinations of PrPC antibodies, different blocking agents, buffers or trace amounts of copper ion did not improve PrPC binding in the A $\beta$ 42 EpiMap ELISA. All epitope mapping results are presented in Table 1.

### The recombinant PrPC and A $\beta$ 42 interaction

The bound PrPC against full-length A $\beta$ 42 was detected. A $\beta$ 42-conjugated beads were incubated with PrPC and were detected by HRP-conjugated T2 antibody using luminescence (Figure 5). This test set ( $41\,040 \pm 1198$  RLU) was significant compared to background where A $\beta$ 42-conjugated ( $3896 \pm 585$  RLU) and BA-conjugated ( $4582 \pm 458$  RLU) beads were treated with HRP-conjugated anti-PrPC ( $P < 0.001$ ). Although little non-specific binding with PrPC and BA was observed ( $15\,309 \pm 1666$  RLU) in the negative control, PrPC and A $\beta$ 42 binding was still found to be significant ( $P < 0.05$ ) compared to the negative control. For the positive control, PrPC-conjugated beads were incubated with HRP-conjugated anti-PrPC ( $64\,804 \pm 533$  RLU).

### DISCUSSION

Antibody epitopes and protein–protein interactions were identified by developing a 96-well-based epitope mapping

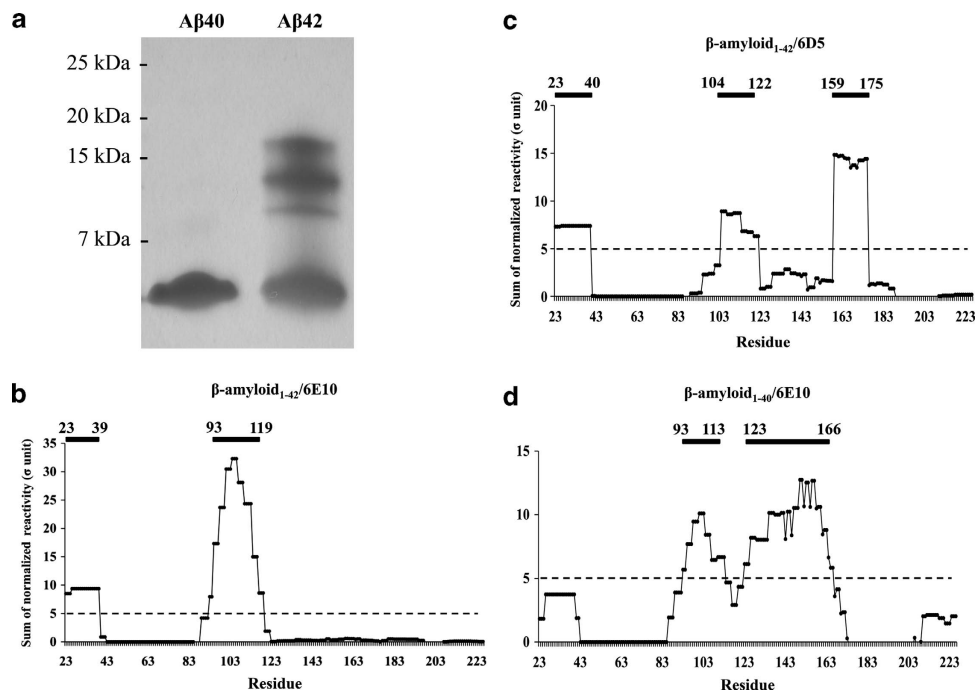


**Figure 4** (a) Electrophoresis of  $\beta$ -amyloid<sub>1–40</sub> (A $\beta$ 40) and  $\beta$ -amyloid<sub>1–42</sub> (A $\beta$ 42). A $\beta$ 42 was used in the cellular prion protein (PrPC) epitope mapping enzyme-linked immunosorbent assay (EpiMap ELISA) and detected by (b) the 6E10 antibody and (c) 6D5 A $\beta$ 42 antibodies. (d) Monomeric A $\beta$ 40 bound to PrPC EpiMap ELISA was detected with the 6E10 antibody. The black bar and the number indicate the binding epitopes of A $\beta$  that were used in the PrPC EpiMap ELISA experiments.

**Table 1 Summary of epitope mapping results by the EpiMap ELISA**

EpiMap ELISA	Protein/antibody	Detection antibody	Reported epitopes	EpiMap ELISA results
PrPC	SAF-32	Anti-mouse IgG-HRP	57–88	26–42 86–103
PrPC	6D11	Anti-mouse IgG-HRP	93–109	89–116
A $\beta$ 42	1E11	Anti-mouse IgG-HRP	1–8	1–15
A $\beta$ 42	4G8-HRP	—	17–24	13–29
PrPC	A $\beta$ 42	6E10-HRP	N-terminus 95–110	23–39 93–119
PrPC	A $\beta$ 42	6D5-Biotin/Avidin-HRP	—	23–40 104–122 159–175
PrPC	A $\beta$ 40	6E10-HRP	—	93–113 123–166
A $\beta$ 42	PrPC	T2-HRP	—	—

Abbreviations: A $\beta$ 40,  $\beta$ -amyloid<sub>1–40</sub>; A $\beta$ 42,  $\beta$ -amyloid<sub>1–42</sub>; EpiMap ELISA, epitope mapping enzyme-linked immunosorbent assay; HRP, horseradish peroxidase; IgG, immunoglobulin G; PrPC, cellular prion protein.

and 20 amino acids, generally); however, no reviews have been published regarding the minimum number of amino acids for peptide–protein interactions. Using shorter peptides with a slight rift between the overlapping peptides increases the resolution of epitope mapping; however, costs may be excessive if the protein is too long.

To avoid steric hindrance, the peptide design should include specific types of spacers at one of the ends. Generally, biotin attaches at the C-termini of peptides with a spacer moiety such as a polyethylene glycol or a GSGS motif. The use of avidin to link biotinylated peptides on the surface of the plate limits its application when biotinylated antibodies are the only viable option. To circumvent this problem, we used a cysteine–maleimide covalent bond to generate strong, irreversible binding for overlapping peptides. Activated-maleimides are attached on the surface through a 12 Å-long linker, followed by Pierce technical support. Therefore, the synthesis of overlapping peptides with spacers was not necessary because only cysteine was attached to one of the ends, except for peptides containing an inner cysteine in PrPC-overlapping peptides (amino acids 179, 214). Overlapping peptides generated from cysteine-containing proteins remove the inner cysteine or replace it with other amino acids for the following reasons: (1) two cysteines in an overlapping peptide may form an inner disulfide bond resulting in a circular peptide; and (2) free cysteines may be coupled to ligands, creating incorrect epitopes. Fundamentally, cysteine residues that are involved in forming the structure do not participate in the protein interaction. Therefore, cysteines in the protein must be substituted by other amino acids; consequently, in our experiments, an inner cysteine in the overlapping peptide was used to conjugate the peptide on a microplate. A review article published in 2004 described efficient and accurate epitope mapping strategies as well as detailed protocols.<sup>48</sup>

The EpiMap ELISA tests were performed rapidly and easily in the laboratory using basic manual or automated standard equipment for ELISA experiments. Peptide-conjugated microplates were prepared and preserved more easily compared to nitrocellulose membranes, which require specific techniques or machines to spot the peptides and were often fragile. Conjugating cysteinyl-overlapping peptides on the microplate was comparable to the same level of difficulty as coating antibodies or proteins for ELISA experiments. Increased hydrophobicity due to the incorporation of the cysteine at the end of the overlapping peptides was the only limitation to these experiments. Synthesis failure occurred in PrPC peptides no. 10, 12, 13, 18, 40 and A $\beta$ 42 peptide no. 15. Several hydrophobic peptides were dissolved in DMSO prior to conjugation to the maleimide-activated microtiter plate. Thus, when dissolving such peptides, the DMSO concentration was considered to be less than 1% (~0.3%) in the final product.

Potentially, cysteinyl peptide dimers formed through their free sulphhydryl groups were reduced through dilution with phosphate buffer (pH 4.5) to protonate-free sulphhydryl groups with hydrogen. The pH after further dilution to 5  $\mu$ g ml<sup>-1</sup> in the dilution buffer was between 6.5 and 7.5, allowing the

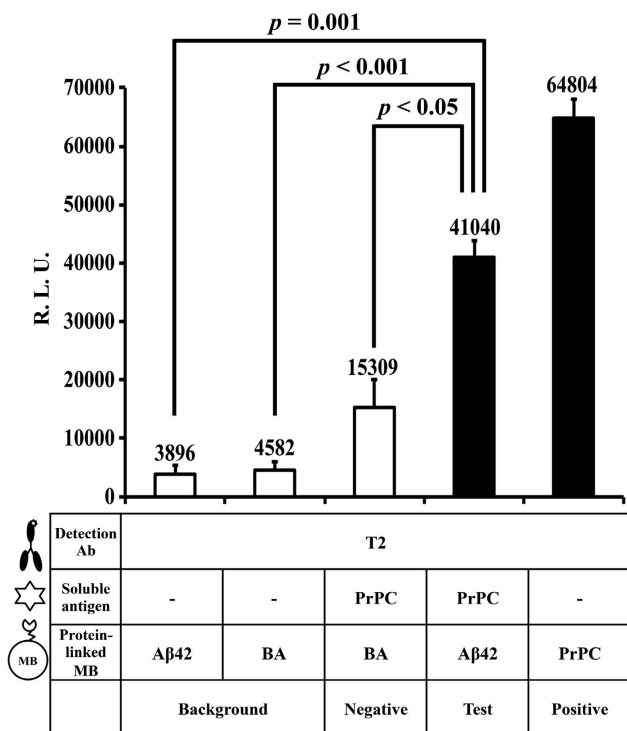


**Figure 5** The precipitation of cellular prion protein (PrPC) by  $\beta$ -amyloid<sub>1–42</sub> (A $\beta$ 42)-conjugated magnetic beads (MB) were detected with the T2 antibody ( $P < 0.05$ ). A $\beta$ 42- and BLOCK ACE (BA)-linked MB were used in the negative controls, and PrPC-coupled MB was the positive control. Ab, antibodies.

ELISA using multiple overlapping peptides. The minimum length for an overlapping peptide is recommended to be at least an 8 mer for antibody epitope mapping (between 8

efficient formation of thioether bonds between the maleimides and the free sulfhydryl groups. Not to mention the long preservation of lyophilized peptides requires the peptides to be maintained in a desiccated freezer to prevent moisture gain.

As Lauren *et al.*<sup>39</sup> reported, the 6D11 PrPC antibody competed with the A $\beta$ 42-binding region. In addition, the PrPC EpiMap ELISA revealed that A $\beta$ 42 also binds to the N-terminal PrPC (amino acids 23–39), which may be due to the high affinity of A $\beta$ 42 towards polybasic residues.<sup>40</sup> Interestingly, the 6E10 antibody directed toward the N-terminus of A $\beta$ 42 detected bound A $\beta$ 42 in the PrPC EpiMap ELISA. The 6D5 antibody (specific to C-terminus of A $\beta$ 42) detected bound A $\beta$ 42 at both the N- and C-termini of the PrPC, which may be attributed to a number of causes; however, one possibility in this experiment may be the diverse conformational interaction between A $\beta$ 42 and PrPC. Nuclear magnetic resonance studies on A $\beta$ 42 suggested that residues 16–21 and 30–40 were located in the core of the fibrils, involving in amyloid assembly.<sup>51–53</sup> Various A $\beta$ 42 oligomeric structures may be as complex as the C-terminus toward the core or staggered A $\beta$ 42  $\beta$ -strands in fibrils.<sup>12</sup> Furthermore, previous studies suggested that A $\beta$ 42 oligomers along with the low molecular weight of A $\beta$ 42 may result in its ability to bind to PrPC, implying that several types of A $\beta$ 42 forms may interact with PrPC.<sup>39,54</sup>

A $\beta$ 40 was also used in the PrPC EpiMap ELISA and was detected by 6E10. In relation to A $\beta$ 40, Pflanzner *et al.*<sup>55</sup> suggested that monomeric A $\beta$ 40 was bound to PrPC at low concentrations. The monomeric form of A $\beta$ 40 that we used bound to PrPC in a similar manner as A $\beta$ 42. Similarities in the 3D structures of A $\beta$ 40 and A $\beta$ 42 are currently unknown and should be investigated in further studies. Overall, A $\beta$ 42 interacted with PrPC independently from different epitopes. Depending on the epitope of the A $\beta$ 42 antibody utilized, A $\beta$ 42 binding to PrPC differed; therefore, their contact interfaces may be diverse or only a monomer from the A $\beta$ 42 multimer was involved in binding PrPC.<sup>42</sup> A $\beta$ 42 and A $\beta$ 40 bound to PrPC; therefore, the A $\beta$ -PrPC interaction may be diverse, suggesting that various structure types of A $\beta$  may be involved in binding.

When PrPC was used in the A $\beta$ 42 EpiMap ELISA experiment, the bound PrPC was not detected with different PrPC antibodies against different epitopes (data not shown). The interaction between PrPC and A $\beta$ 42 may be dependent on the 3D conformation of the A $\beta$ 42 oligomers. Therefore, the linear peptides used in the A $\beta$ 42 EpiMap ELISA did not bind to PrPC. Recombinant PrPC and A $\beta$ 42 that were prepared in diverse oligomeric forms interacted efficiently in a bead-based ELISA, suggesting that possible interactions occur when the proteins are in their 3D structure. However, overlapping peptide no. 15 failed in the synthesis of the A $\beta$ 42 EpiMap ELISA, which resulted in the absence of amino acid 42. In protein interactions, one amino acid may be critical in determining the overall interaction, but no evidence was elucidated regarding whether this last amino acid has an important role in binding PrPC.

In conclusion, EpiMap ELISAs for PrPC and A $\beta$ 42 were developed to map the binding of epitopes with interactomes.

Residues 23–39 and 93–119 of the PrPC sequence were important in A $\beta$ 42 binding. These two regions interacted with A $\beta$ 42 oligomers independently; however, their synergetic effect was not tested. In addition, 6E10 (against N-terminal A $\beta$ 42) and 6D5 (against C-terminal A $\beta$ 42) detected bound A $\beta$ 42 on the PrPC EpiMap ELISA, suggesting that A $\beta$ 42 interacted with PrPC in a diverse manner. The binding of the A $\beta$ 40 monomer with PrPC was reported in a previous publication,<sup>55</sup> and similar A $\beta$ 40 monomer binding sites were found, which suggests the possible role of A $\beta$ 40 conformations in the interaction with PrPC. Conversely, PrPC in the A $\beta$ 42 EpiMap ELISA did not identify binding epitopes, which was thought to be caused by 3D conformation-dependent binding for A $\beta$ 40 and A $\beta$ 42.

Studies regarding PrPC binding to A $\beta$ 42 have utilized various methods that require genetic engineering or other laborious techniques. Our study identified protein interaction sites using the EpiMap ELISA, suggesting an easy platform that can be used to determine various binding sites of proteins within as little as 3 h. Our identification of the interaction sites of PrPC with A $\beta$  may be useful in therapeutic research for blockers or mimics against PrPC or A $\beta$ . Recently, PrPC and A $\beta$  interactions have shown to activate Fyn kinase in AD.<sup>56</sup> Therefore, PrPC and A $\beta$  interactions are important for the understanding of toxic mechanisms of A $\beta$  oligomers, which should first be established to target these mechanisms in pharmaceutical interventions in AD.

## CONFLICT OF INTEREST

The authors declare no conflict of interest.

## ACKNOWLEDGEMENTS

This study was funded by the Korea Centers for Disease Control & Prevention, Ministry of Health & Welfare (2011-E53001-00) and the National Research Foundation of Korea (2012R1A1A2A04).

- 1 Prusiner SB. Prions. *Proc Natl Acad Sci USA* 1998; **95**: 13363–13383.
- 2 Ross CA, Poirier MA. Protein aggregation and neurodegenerative disease. *Nat Med* 2004; **10** (Suppl): S10–S17.
- 3 Prusiner SB, Hsiao KK. Human prion diseases. *Ann Neurol* 1994; **35**: 385–395.
- 4 Bueller H, Fischer M, Lang Y, Bluethmann H, Lipp HP, DeArmond SJ *et al.* Normal development and behaviour of mice lacking the neuronal cell-surface PrP protein. *Nature* 1992; **356**: 577–582.
- 5 Manson JC, Clarke AR, Hooper ML, Aitchison L, McConnell I, Hope J. 129/Ola mice carrying a null mutation in PrP that abolishes mRNA production are developmentally normal. *Mol Neurobiol* 1994; **8**: 121–127.
- 6 Turnbaugh JA, Westergard L, Unterberger U, Biasini E, Harris DA. The N-terminal, polybasic region is critical for prion protein neuroprotective activity. *PLoS One* 2011; **6**: e25675.
- 7 Bounhar Y, Zhang Y, Goodyer CG, LeBlanc A. Prion protein protects human neurons against Bax-mediated apoptosis. *J Biol Chem* 2001; **276**: 39145–39149.
- 8 Roucou X, Giannopoulos PN, Zhang Y, Jodoin J, Goodyer CG, LeBlanc A. Cellular prion protein inhibits proapoptotic Bax conformational change in human neurons and in breast carcinoma MCF-7 cells. *Cell Death Differ* 2005; **12**: 783–795.
- 9 Brown DR, Schulz-Schaeffer WJ, Schmidt B, Kretzschmar HA. Prion protein-deficient cells show altered response to oxidative stress due to decreased SOD-1 activity. *Exp Neurol* 1997; **146**: 104–112.



- 10 Brown DR, Nicholas RS, Canevari L. Lack of prion protein expression results in a neuronal phenotype sensitive to stress. *J Neurosci Res* 2002; **67**: 211–224.
- 11 Kim BH, Lee HG, Choi JK, Kim JI, Choi EK, Carp RI *et al*. The cellular prion protein (PrP<sup>C</sup>) prevents apoptotic neuronal cell death and mitochondrial dysfunction induced by serum deprivation. *Brain Res Mol Brain Res* 2004; **124**: 40–50.
- 12 Ahmed M, Davis J, Aucoin D, Sato T, Ahuja S, Aimoto S *et al*. Structural conversion of neurotoxic amyloid-beta(1-42) oligomers to fibrils. *Nat Struct Mol Biol* 2010; **17**: 561–567.
- 13 Christensen HM, Harris DA. Prion protein lacks robust cytoprotective activity in cultured cells. *Mol Neurodegener* 2008; **3**: 11.
- 14 Selkoe DJ. Biochemistry and molecular biology of amyloid beta-protein and the mechanism of Alzheimer's disease. *Handb Clin Neurol* 2008; **89**: 245–260.
- 15 Tam JH, Pasternak SH. Amyloid and Alzheimer's disease: inside and out. *Can J Neurol Sci* 2012; **39**: 286–298.
- 16 Walsh DM, Selkoe DJ. Deciphering the molecular basis of memory failure in Alzheimer's disease. *Neuron* 2004; **44**: 181–193.
- 17 Gouras GK, Tampellini D, Takahashi RH, Capetillo-Zarate E. Intraneuronal beta-amyloid accumulation and synapse pathology in Alzheimer's disease. *Acta Neuropathol* 2010; **119**: 523–541.
- 18 Busciglio J, Pelsman A, Wong C, Pigino G, Yuan M, Mori H *et al*. Altered metabolism of the amyloid beta precursor protein is associated with mitochondrial dysfunction in Down's syndrome. *Neuron* 2002; **33**: 677–688.
- 19 Cataldo AM, Petanceska S, Terio NB, Peterhoff CM, Durham R, Mercken M *et al*. Abeta localization in abnormal endosomes: association with earliest Abeta elevations in AD and Down syndrome. *Neurobiol Aging* 2004; **25**: 1263–1272.
- 20 D'Andrea MR, Nagele RG, Wang HY, Peterson PA, Lee DH. Evidence that neurons accumulating amyloid can undergo lysis to form amyloid plaques in Alzheimer's disease. *Histopathology* 2001; **38**: 120–134.
- 21 Echeverria V, Cuervo AC. Intracellular A-beta amyloid, a sign for worse things to come? *Mol Neurobiol* 2002; **26**: 299–316.
- 22 Gouras GK, Tsai J, Naslund J, Vincent B, Edgar M, Checler F *et al*. Intraneuronal Abeta42 accumulation in human brain. *Am J Pathol* 2000; **156**: 15–20.
- 23 Ohnogi Y, Asahara H, Chui DH, Tsuruta Y, Sakae N, Miyoshi K *et al*. Intracellular Abeta42 activates p53 promoter: a pathway to neurodegeneration in Alzheimer's disease. *FASEB J* 2005; **19**: 255–257.
- 24 De Strooper B. Proteases and proteolysis in Alzheimer disease: a multifactorial view on the disease process. *Physiol Rev* 2010; **90**: 465–494.
- 25 Hardy JA, Higgins GA. Alzheimer's disease: the amyloid cascade hypothesis. *Science* 1992; **256**: 184–185.
- 26 Hardy J, Selkoe DJ. The amyloid hypothesis of Alzheimer's disease: progress and problems on the road to therapeutics. *Science* 2002; **297**: 353–356.
- 27 Lee HG, Zhu X, Castellani RJ, Nunomura A, Perry G, Smith MA. Amyloid-beta in Alzheimer disease: the null versus the alternate hypotheses. *J Pharmacol Exp Ther* 2007; **321**: 823–829.
- 28 Ashe KH, Zahs KR. Probing the biology of Alzheimer's disease in mice. *Neuron* 2010; **66**: 631–645.
- 29 Caughey B, Lansbury PT. Protofibrils, pores, fibrils, and neurodegeneration: separating the responsible protein aggregates from the innocent bystanders. *Annu Rev Neurosci* 2003; **26**: 267–298.
- 30 Haass C, Selkoe DJ. Soluble protein oligomers in neurodegeneration: lessons from the Alzheimer's amyloid beta-peptide. *Nat Rev Mol Cell Biol* 2007; **8**: 101–112.
- 31 Klein WL, Krafft GA, Finch CE. Targeting small Abeta oligomers: the solution to an Alzheimer's disease conundrum? *Trends Neurosci* 2001; **24**: 219–224.
- 32 Ferreira ST, Vieira MN, De Felice FG. Soluble protein oligomers as emerging toxins in Alzheimer's and other amyloid diseases. *IUBMB life* 2007; **59**: 332–345.
- 33 Dong S, Duan Y, Hu Y, Zhao Z. Advances in the pathogenesis of Alzheimer's disease: a re-evaluation of amyloid cascade hypothesis. *Transl Neurodegener* 2012; **1**: 18.
- 34 Chakravarthy B, Menard M, Ito S, Gaudet C, Dal Pra I, Armato U *et al*. Hippocampal membrane-associated p75NTR levels are increased in Alzheimer's disease. *J Alzheimers Dis* 2012; **30**: 675–684.
- 35 Shankar GM, Bloodgood BL, Townsend M, Walsh DM, Selkoe DJ, Sabatini BL. Natural oligomers of the Alzheimer amyloid-beta protein induce reversible synapse loss by modulating an NMDA-type glutamate receptor-dependent signaling pathway. *J Neurosci* 2007; **27**: 2866–2875.
- 36 Magdesian MH, Carvalho MM, Mendes FA, Saraiva LM, Juliano MA, Juliano L *et al*. Amyloid-beta binds to the extracellular cysteine-rich domain of Frizzled and inhibits Wnt/beta-catenin signaling. *J Biol Chem* 2008; **283**: 9359–9368.
- 37 De Felice FG, Vieira MN, Bomfim TR, Decker H, Velasco PT, Lambert MP *et al*. Protection of synapses against Alzheimer's-linked toxins: insulin signaling prevents the pathogenic binding of Abeta oligomers. *Proc Natl Acad Sci USA* 2009; **106**: 1971–1976.
- 38 Benilova I, De Strooper B. Prion protein in Alzheimer's pathogenesis: a hot and controversial issue. *EMBO Mol Med* 2010; **2**: 289–290.
- 39 Lauren J, Gimbel DA, Nygaard HB, Gilbert JW, Strittmatter SM. Cellular prion protein mediates impairment of synaptic plasticity by amyloid-beta oligomers. *Nature* 2009; **457**: 1128–1132.
- 40 Chen S, Yadav SP, Surewicz WK. Interaction between human prion protein and amyloid-beta (Abeta) oligomers: role OF N-terminal residues. *J Biol Chem* 2010; **285**: 26377–26383.
- 41 Kessels HW, Nguyen LN, Nabavi S, Malinow R. The prion protein as a receptor for amyloid-beta. *Nature* 2010; **466**: E3–E4. (discussion E-5).
- 42 Gallion SL. Modeling amyloid-beta as homogeneous dodecamers and in complex with cellular prion protein. *PLoS One* 2012; **7**: e49375.
- 43 Frank R. The SPOT-synthesis technique. Synthetic peptide arrays on membrane supports—principles and applications. *J Immunol Methods* 2002; **267**: 13–26.
- 44 Geysen HM, Rodda SJ, Mason TJ, Tribbick G, Schoofs PG. Strategies for epitope analysis using peptide synthesis. *J Immunol Methods* 1987; **102**: 259–274.
- 45 Rodda SJ, Tribbick G. Antibody-defined epitope mapping using the multipin method of peptide synthesis. *Methods* 1996; **9**: 473–481.
- 46 Zahn R, von Schroetter C, Wuthrich K. Human prion proteins expressed in *Escherichia coli* and purified by high-affinity column refolding. *FEBS Lett* 1997; **417**: 400–404.
- 47 Hayashi H, Takata M, Iwamaru Y, Ushiki Y, Kimura KM, Tagawa Y *et al*. Effect of tissue deterioration on postmortem BSE diagnosis by immunobiochemical detection of an abnormal isoform of prion protein. *J Vet Med Sci* 2004; **66**: 515–520.
- 48 Carter JM, Loomis-Price L. B cell epitope mapping using synthetic peptides. In Coligan JE (ed.). *Current Protocols in Immunology* 2004. (Chapter 9:Unit 9 4).
- 49 Feraudet C, Morel N, Simon S, Volland H, Frobert Y, Creminon C *et al*. Screening of 145 anti-PrP monoclonal antibodies for their capacity to inhibit PrPSc replication in infected cells. *J Biol Chem* 2005; **280**: 11247–11258.
- 50 Spinner DS, Kascsak RB, Lafauci G, Meeker HC, Ye X, Flory MJ *et al*. CpG oligodeoxynucleotide-enhanced humoral immune response and production of antibodies to prion protein PrPSc in mice immunized with 139A scrapie-associated fibrils. *J Leukoc Biol* 2007; **81**: 1374–1385.
- 51 Petkova AT, Ishii Y, Balbach JJ, Antzutkin ON, Leapman RD, Delaglio F *et al*. A structural model for Alzheimer's beta-amyloid fibrils based on experimental constraints from solid state NMR. *Proc Natl Acad Sci USA* 2002; **99**: 16742–16747.
- 52 Torok M, Milton S, Kaye R, Wu P, McIntire T, Glabe CG *et al*. Structural and dynamic features of Alzheimer's Abeta peptide in amyloid fibrils studied by site-directed spin labeling. *J Biol Chem* 2002; **277**: 40810–40815.
- 53 Sanchez de Groot N, Pallares I, Aviles FX, Vendrell J, Ventura S. Prediction of "hot spots" of aggregation in disease-linked polypeptides. *BMC Struct Biol* 2005; **5**: 18.
- 54 Calella AM, Farinelli M, Nuvolone M, Mirante O, Moos R, Falsig J *et al*. Prion protein and Abeta-related synaptic toxicity impairment. *EMBO Mol Med* 2010; **2**: 306–314.
- 55 Pflanzner T, Petsch B, Andre-Dohmen B, Muller-Schiffmann A, Tschickardt S, Weggen S *et al*. Cellular prion protein participates in amyloid-beta transcytosis across the blood-brain barrier. *J Cereb Blood Flow Metab* 2012; **32**: 628–632.
- 56 Um JW, Strittmatter SM. Amyloid- $\beta$  induced signaling by cellular prion protein and Fyn kinase in Alzheimer disease. *Prion* 2013; **7**: 37–41.



This work is licensed under a Creative Commons Attribution-NonCommercial-NoDerivs 3.0 Unported License. To view a copy of this license, visit <http://creativecommons.org/licenses/by-nc-nd/3.0/>